



LATERAL TORSIONAL BUCKLING ANALYSIS AND DESIGN OF STEEL BEAMS WITH CONTINUOUS SPANS

Sahraei, Arash¹, Pezeshky, Payam² and Mohareb, Magdi^{3,4}

¹ Graduate research assistant, University of Ottawa, Canada

² Graduate research assistant, University of Ottawa, Canada

³ Professor, University of Ottawa, Canada

⁴ MagdiEmile.Mohareb@uottawa.ca

Abstract:

Design standards do not provide provisions to account for the interaction between adjacent spans of continuous beams. In the absence of such provisions, the designer may opt for calculating the lateral torsional buckling capacity for each span separately by applying the moment gradient factors provided in standards and adopting the smallest critical moment as the one governing the design. The Salvadori hypothesis of isolating a member from the rest of the structure is assessed in the present study. The elastic lateral torsional buckling resistance for continuous beams is investigated based on finite element analysis. Comparisons are made between two types of solutions: (1) those neglecting interaction effects between adjacent spans, and (2) those considering span interaction. Also examined is the effect of presence of lateral/torsional restraints at intermediate supports of continuous beams. The results illustrate the merits of adopting the FEA solution in accounting for span interaction when determining the elastic lateral torsional buckling capacity of continuous beams.

Keywords: lateral torsional buckling, finite element analysis, interaction effects, moment gradient factors, continuous beams

1. INTRODUCTION AND LITERATURE REVIEW

Present provisions in design standards (e.g., CAN/CSA-S16-14 (2014), EN 1993 Designer's guide (Gardner and Nethercot 2011), AS-4100 (1998) and ANSI/AISC-360-16 (2016)) do not account for the interaction between various segments of a continuous beam when determining their lateral torsional buckling (LTB) resistance. In the absence of such provisions, designers may resort to treating each segment as a separate span and calculate the individual LTB capacity for each segment separately by adopting moment gradient factors and critical moment equations provided in standards, and then, conservatively, adopt the smallest critical moment as the one governing the LTB capacity of the continuous beam. The above procedure omits the interaction effect between adjacent members. Procedures that account for such interaction effects were proposed in the work of (Nethercot and Trahair 1976), (Trahair 1977) and (Trahair and Bradford 1988) as reported in SSRC guide (Ziemian 2010). Such procedures are iterative and based on an analogy between the LTB buckling of continuous beams and flexural buckling of continuous columns. According to (Ziemian 2010), in most cases, these procedures lead to conservative estimates for the critical moments while in cases of high moment gradients, they can overestimate the LTB buckling strength. The present study documents a LTB Finite Element Analysis (FEA) that captures

interaction effects in continuous beams. To establish the validity of the FEA model, the FEA is first adopted to determine the critical moments for a number of single span problems under a variety of loads and comparisons are made against the critical moment predicted by design standard provisions. The finite element is then adopted to investigate the span interaction effect on the lateral torsional buckling of continuous beams and identify conditions where interaction effects are significant. The model is then used to quantify the effect of lateral and torsional restraints that may be present at intermediate supports.

2. OVERVIEW OF FINITE ELEMENT FORMULATION

The formulation is based on the following assumptions:

1. Material is linearly elastic, isotropic and homogenous.
2. The beam follows the Vlasov beam kinematics (Vlasov 1961), i.e., the section is assumed to move in its own plane as a rigid disk and the shear strain in the middle surface of the beam is negligible.
3. Pre-buckling deformations and local warping effects are neglected.

The beam finite element in (Barsoum and Gallagher 1970) is chosen to conduct the study. The element has two nodes, each having three pre-buckling and four buckling degrees of freedom (DOF) as shown in Figure 1a. The pre-buckling DOFs are the longitudinal displacement u , the transverse displacement w and the strong-axis rotation w' and the buckling displacements are the lateral displacement v , the weak-axis rotation v' , the angle of twist θ_x and warping deformation θ'_x . In Figure 1a, displacements are shown with red single arrows, rotations are depicted with blue double-headed arrows while the warping displacements are illustrated by green triple-headed arrows.

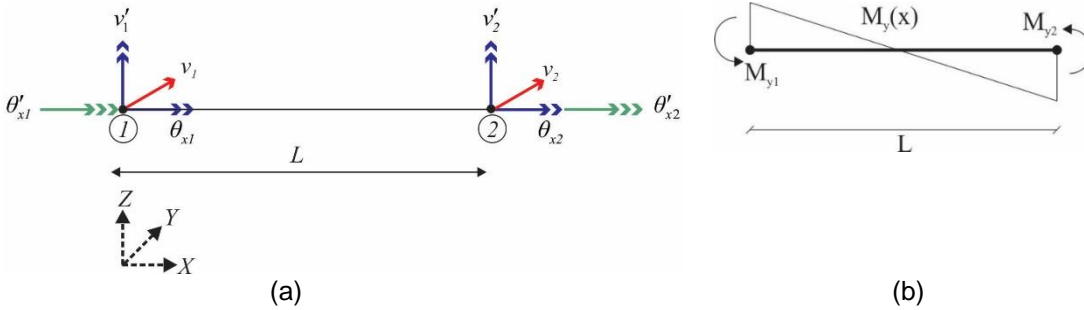


Figure 1: (a) Buckling DOFs and adopted right-handed coordinate system, and (b) Internal force interpolation bending moment

The strong-axis bending moments M_{y1} and M_{y2} at the ends of each member are obtained from the pre-buckling analysis. Assuming the beam element length L is small, the bending moments within the element are linearly interpolated (Figure 1b), i.e., $M_y(x) \approx [-M_{y1}(1 - x/L) + M_{y2}(x/L)]$. The total potential energy in going from the point of onset of buckling to the buckled configuration is expressed in terms of buckling displacements as

$$[1] \quad \Pi_{eb} = U_b + V_b = (U_v + U_{sv} + U_w) + (V_m + V_{PL} + V_{qL})$$

where the internal strain energy U_b is the sum of three components; U_v due to the lateral displacement v , U_{sv} due to the conventional Saint-Venant torsion, and U_w due to warping torsion. Also, the destabilizing load potential energy term V_b consists of three components; V_m due to the bending moments, V_{PL} due to the load height above the shear centre for point loads, and V_{qL} is load height effect above the shear centre for line loads. By expressing the above six terms in terms of the lateral displacement v and the angle of twist θ_x , one obtains

$$[2] \quad \Pi_{eb} = \left(\frac{1}{2} \int_0^L EI_z (v'')^2 dx + \frac{1}{2} \int_0^L GJ \theta_x'^2 dx + \frac{1}{2} \int_0^L EC_w \theta_x''^2 dx \right) + \lambda \left(\int_0^L M_y(x) \theta_x v'' dx + \sum_{i=1}^{np} \frac{1}{2} P_i z_i \theta_x^2 + \frac{1}{2} \int_0^L q(x) z_q \theta_x^2 dx \right)$$

where G is the shear modulus, J is the Saint-Venant torsional constant, I_z is weak-axis moment of inertia, C_w is the warping constant, z_i is the vertical distance between the section shear centre and the point of application of transverse load P_i ($i = 1, \dots, np$) taken as positive in the positive direction of coordinate z , $q(x)$ is the member transverse line load, and z_q is the vertical distance between the shear centre and the line of application for $q(x)$, taken positive in the positive direction of coordinate z . The lateral displacement $v(x)$ and angle of twist $\theta_x(x)$ are related to the nodal displacements using Hermitian polynomials. By substituting into Eq. [2] and evoking the stationarity conditions, one obtains the linearized eigenvalue problem:

$$[3] \quad ([K] - \lambda [K_G]) \{U\} = \{0\}$$

where $[K]$ is the elastic stiffness matrix, $[K_G]$ is the geometric stiffness matrix, the eigenvalue λ is a load multiplier that determines the buckling load(s) at the which the system buckles and the eigen vector $\{U\}$ is the buckling configuration.

3. VALIDATION STUDY

Three beam geometries were considered to assess the validity of the FEA. These are: 1) a W410x39 with a 4.5m span, 2) a W410x39 with an 8m span, and 3) a W310x52 with a 5.7m span. All beams were simply supported with respect to the lateral displacement and twist (i.e., $v(0) = v(L) = \theta_x(0) = \theta_x(L) = 0$, but free to undergo weak-axis rotation and warping, i.e., $v'(0) \neq 0, v'(L) \neq 0, \theta_x'(0) \neq 0, \theta_x'(L) \neq 0$ as may be the case in beams connected to columns through simple shear connections. A variety of loading conditions were investigated; end moments ($M, \psi M$), where $\psi = 1, 0.75, 0.5, 0.25, 0, -0.25, -0.5, -0.75, -1$ (runs #1-9), uniformly distributed loads with and without fixed end moments (runs #10, 11), mid-span point load with and without fixed end moments (runs #12, 13), and two point loads acting at third spans (run #14). A mesh study indicated that eight finite elements are needed to achieve convergence. Thus, eight elements were used to mesh all beams. In each case, the critical moments $M_{cr} = M_{cr}(FEA)$ based on FEA were computed and the corresponding moment gradient $C = C(FEA)$ was determined from the equation

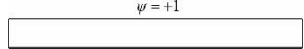
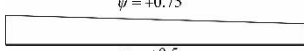
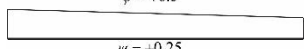
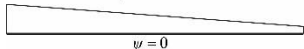
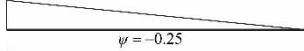
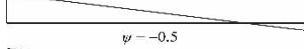
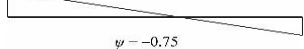
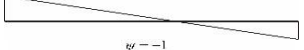


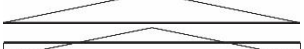

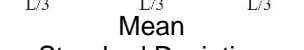
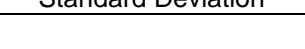
$$[4] \quad M_{cr} = CM_u = C \frac{\pi}{L} \sqrt{EI_y GJ + (\pi E/L)^2 C_w I_y}$$

where $M_u = (\pi/L) \sqrt{EI_y GJ + (\pi E/L)^2 C_w I_y}$ is the critical moment for the idealized case of a simply supported beam ($v(0) = \theta_x(0) = v(L) = \theta_x(L) = 0$) subjected to uniform moments. The corresponding moment gradient values are provided in Column 2 of Table 1. The critical moment expression in Equation [4] is universal in most standards. For example, the Eurocode guide adopts equation [4] in conjunction with moment gradient factors $C = C(EUR)$ prescribed for various loading conditions as provided in Column 3 of Table 1. Also, the Canadian standards CAN/CSA-S16-14 adopt equation [4] with a moment gradient factor $C = C(CAN) = \omega_2$ given by

$$[5] \quad C(CAN) = \left(4M_{\max} / \sqrt{M_{\max}^2 + 4M_a^2 + 7M_b^2 + 4M_c^2} \right) \leq 2.5$$

where M_a, M_b, M_c are moments at the quarter, mid-span, and three-quarter span points, and M_{\max} is the peak moment within the span. The corresponding values are provided in Column (5) of Table 1. The ratios $C(EUR)/C(FAE)$ of the moment gradient factors of the Eurocode guide to those predicted by the FEA are provided in Column (4) and show close agreement except for run #11 and to a lesser degree for run #13, both involving fixed end moments. A comparison for $C(CAN)/C(FAE)$ is provided in Column (6). The mean value of $C(CAN)/C(FAE)$ is 0.936 with a standard deviation 0.0703. In all cases, except run #14, the Canadian moment gradient equation tends to under-predict the critical moments compared to the FEA results.

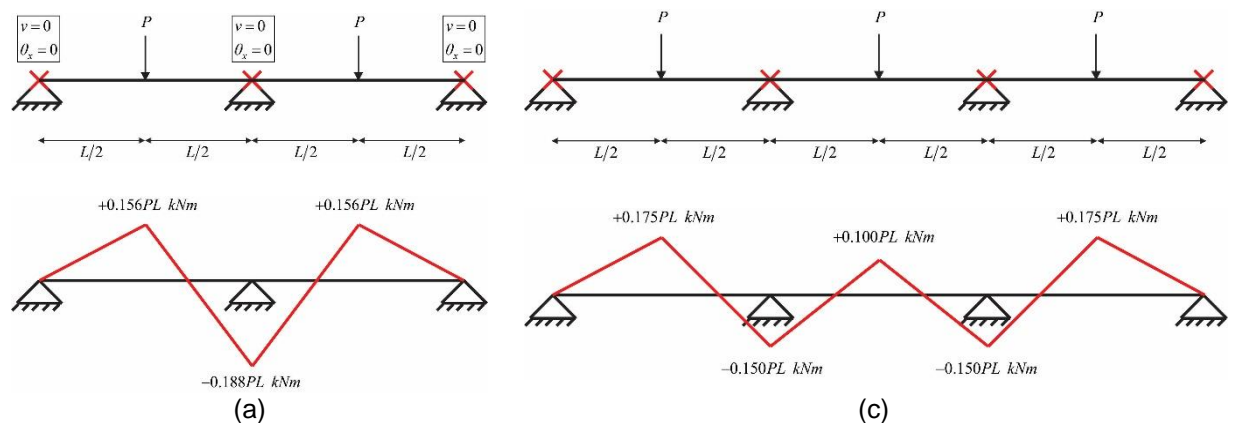
Table 1: Comparison of MFG of FEA, CAN/CSA-S16-14 and EN 1993

Run # (1)	Bending Moment Pattern	$C(FAE)$ Average value of FEA (2)	$C(EUR)$ (3)	$C(EUR) / C(FAE)$ (4)	$C(CAN)$ (5)	$C(CAN) / C(FAE)$ (6)
(1)		1.000	1.000	1.000	1.000	1.000
(2)		1.140	1.141	1.001	1.131	0.992
(3)		1.320	1.323	1.002	1.293	0.980
(4)		1.548	1.563	1.010	1.497	0.967
(5)		1.854	1.879	1.013	1.746	0.942
(6)		2.186	2.281	1.043	2.028	0.928
(7)		2.556	2.704	1.058	2.286	0.894
(8)		2.821	2.927	1.038	2.405	0.853
(9)		2.720	2.752	1.012	2.309	0.849
(10)		1.144	1.132	0.990	1.130	0.988
(11)		2.694	1.285	0.477	2.359	0.876
(12)		1.362	1.365	1.002	1.265	0.929
(13)		1.723	1.565	0.908	1.414	0.821
(14)		1.040	1.046	1.006	1.131	1.088
---	Mean	N/A	N/A	0.969	N/A	0.936
---	Standard Deviation	N/A	N/A	0.140	N/A	0.0703

4. CASE STUDY 1: DEVELOPING DESIGN AIDS FOR CONTINUOUS BEAMS

Consider four continuous beams with equal spans where the spans L vary in the range $L = (4, 5, 6, 7, 8m)$. Beam cross-section in all cases are W250x58 with the properties ($I_{yy} = 1.88 \times 10^{-5} m^4, J = 4.09 \times 10^{-7} m^4, C_w = 2.68 \times 10^{-7} m^6$). All supports provide lateral and torsional

restraints (as marked by the red X) in addition to a transverse restraint. Case (a) involves two spans and is subjected to mid-span point loads P (Figure 2a). Case (b) involves two spans and is subjected to a uniformly distributed load (UDL) (Figure 2b). Case (c) involves three spans and is subjected to mid-span point loads P (Figure 2c) and Case (d) involves three spans and is subjected to UDL (Figure 2d). The pertinent bending moment diagrams (BMD) are shown below each Case. All loads are applied at the shear centre. It is required to determine the critical moment in each case, and use the results to develop design aids by developing moment gradient factors or effective length factors. In a manner similar to the validation study, the moment gradient factor $C(FEA)$ is obtained from the FEA predicted critical moment $M_{cr}(FEA)$ through the relation $C(FEA) = M_{cr}(FEA) / \left[(\pi/L) \sqrt{EI_y GJ + (\pi E/L)^2 C_w I_y} \right]$. Alternatively, one can obtain the effective length factor by solving the equation $M_{cr}(FEA) = (\pi/kL) \sqrt{EI_y GJ + (\pi E/kL)^2 C_w I_y}$ for k . Figure 3a depicts the relationship between the moment gradient factor $C(FEA)$ and the torsion parameter $\chi = L \sqrt{GJ/EC_w}$ and Figure 3b depicts the relationship of the effective length factor k versus the torsion parameter χ . The results show that the moment gradient factors are nearly constant, suggesting the independence of moment gradient of the torsion parameter. In contrast, the effective length factors show a mild dependence on the section torsional parameter. This observation suggests that the moment gradient factor provides a simpler approach to estimate the critical moments than effective length approach. The values provided in Table 2 show that the moment gradient factors is constant for Case (a). Thus a value of $C=1.82$ is recommended for Case (a). In a similar manner, the recommended moment gradient factor is 2.29 for Case (b). Cases (c) and (d) show a rather weak dependence on the torsion parameter, and the smallest values of 1.65 are recommended for Case (c) and 1.75 for Case (d). For run #11 involving three spans with $L=4\text{m}$, the critical moment based on the Canadian Standard equation is 515.3 kNm for the exterior span and 736.3 kNm for the intermediate span. Since there is no direct means of accounting for span interaction in the standards, the critical moment is conservatively taken as the smaller value of 515.3 kNm. This value compares to 891.4 kNm based on FEA. As expected, the FEA solution predicts a higher critical moment since (a) it accounts for interaction effects whereby the stronger span delays the buckling of the weaker span, and (b) the moment gradient equation in the standard is only approximate. For Run #1 involving two-spans with $L=4\text{m}$, the critical moment for both spans predicted by the Canadian Standard equation is 515.2 kNm. An identical value is obtained by modeling a single span, suggesting no interaction effects between identical spans under identical loads. This value compares to 704.9 kNm as predicted by the present FEA solution, suggesting that for the present loads, the CAN-CSA-S16-14 moment gradient equation provides an overly conservative critical moment prediction.



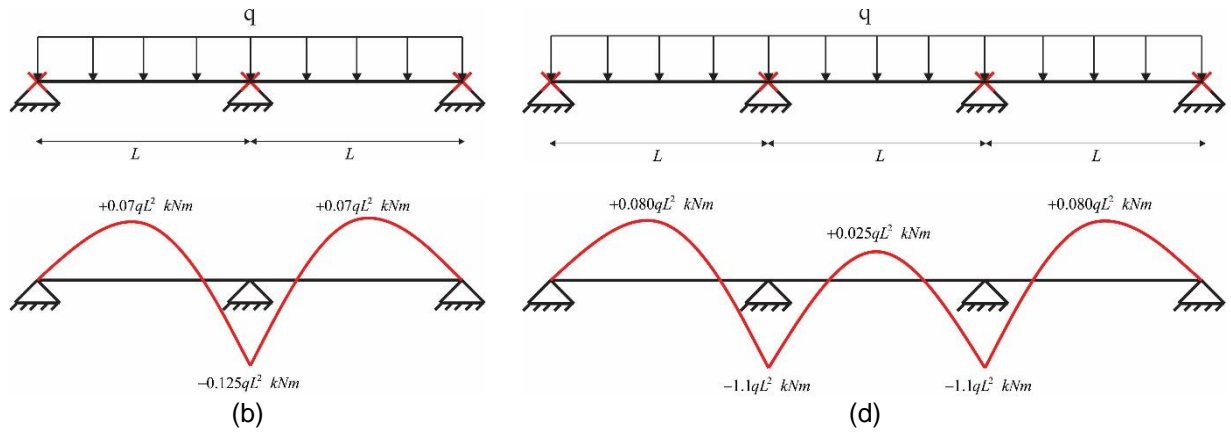


Figure 2: Continuous beams of Example 1: (a) Two-span beams under mid-span point loads, (b) Two-span beams under UDL, (c) three-span beam under mid-span point loads, and (d) three-span beam under UDL

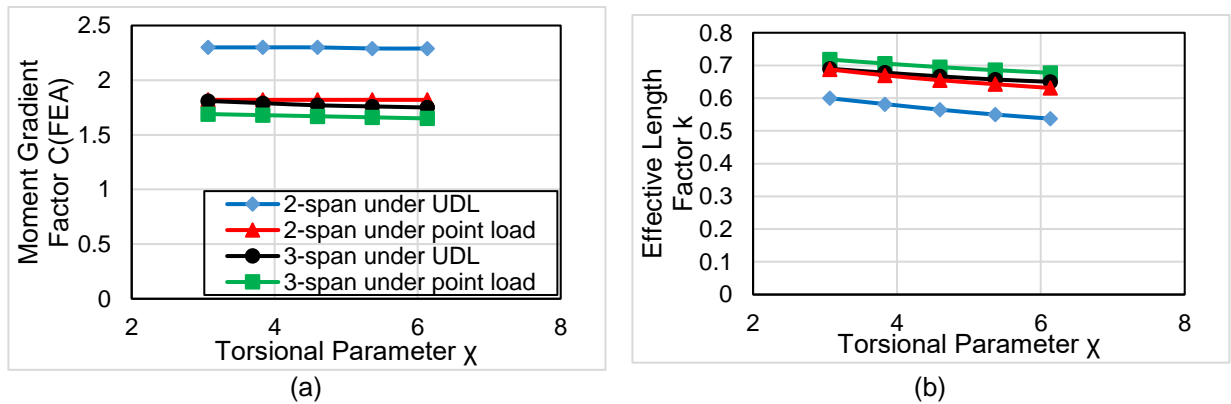


Figure 3: (a) Moment gradient factor vs χ , and (b) Effective length factor vs χ

Run #5 is chosen to illustrate the remaining steps of the design. Given that the W250x58 cross-section meets class 2 requirements for a yield strength $F_y = 350\text{MPa}$, the plastic moment is calculated as $M_p = Z_x F_y = 270\text{kNm}$. For run #5, the critical moment is $M_u = 275.6\text{kNm}$ (Table 2). Given that $M_u < 0.67M_p$, the design is governed by inelastic lateral torsional buckling and the resistance is given by $M_r = \phi M_p (1 - 0.28 M_p / M_u) = 174.8\text{kNm} \leq \phi M_p$. If one assumes the service dead load P_D is equal to the service live load P_L , one has $P = 1.25P_D + 1.5P_L = 2.75P_L$ or $P_L = 0.364P$. The peak factored moment corresponding to P as provided in Figure 2a is $M_f = 0.188PL$. Equating the resisting moment $M_r = 174.8\text{kNm}$ to the factored moment $M_f = 0.188PL$ yields a factored load $P = 116\text{kN}$ which corresponds to a service live load $P_L = 0.364P = 42.2\text{kN}$. The corresponding peak displacement within the span is found as $\Delta = 11.3\text{mm}$ which corresponds to $L/\Delta = 708$ which is lower than the threshold value of $L/\Delta = 360$ given in appendix D of CAN-CSA-S16-14, i.e., the live load deflection meets the requirement of Appendix D.

Table 2: Summarized results of Example 1

Case	Run #	Span (m)	λ	Critical moment (kNm)	$C(FEA)$	k
(a)	1	4	3.07	704.9	1.82	0.688
	2	5	3.83	508.9	1.82	0.670
	3	6	4.60	396.8	1.82	0.655
	4	7	5.37	325.1	1.82	0.643
	5	8	6.13	275.6	1.82	0.631
(c)	6	4	3.07	655.4	1.69	0.718
	7	5	3.83	469.8	1.68	0.706
	8	6	4.60	364.0	1.67	0.695
	9	7	5.37	296.4	1.66	0.686
	10	8	6.13	249.9	1.65	0.678
(b)	11	4	3.07	891.4	2.30	0.600
	12	5	3.83	643.2	2.30	0.582
	13	6	4.60	501.3	2.30	0.565
	14	7	5.37	410.6	2.29	0.550
	15	8	6.13	347.9	2.29	0.538
(d)	16	4	3.07	699.9	1.81	0.690
	17	5	3.83	500.4	1.79	0.678
	18	6	4.60	386.8	1.77	0.667
	19	7	5.37	314.5	1.76	0.657
	20	8	6.13	264.9	1.75	0.650

5. CASE STUDY 2: INTERACTION EFFECTS IN CONTINUOUS BEAMS WITH UNEQUAL SPANS

Consider a continuous beam with a W250x58 cross-section subjected to loads (P_1, P_2, P_3) as shown in Figure 4a. The beam is laterally and torsionally restrained at the three support locations. It is required to determine the elastic LTB capacity of the beam. Two types of solutions are sought: (1) Neglecting interaction effects between both spans and (2) Considering interaction effects.

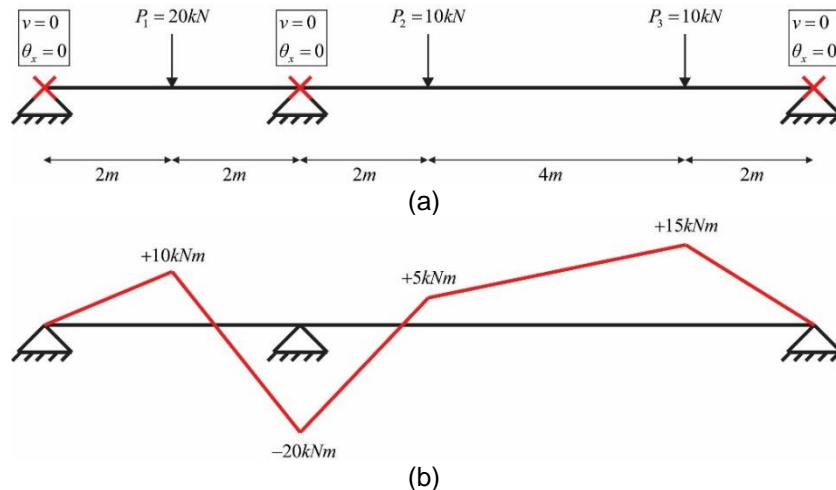


Figure 4: (a) Continuous beam restrained laterally and torsionally at all three supports, and (b) BMD under applied loads

Solution (1) - Omitting interaction: Since CAN/CSA-S16-14 does not account for the interaction between both spans, the designer may opt to calculate the LTB capacity of each span separately by applying the

moment gradient factors based on the quarter-point formula (Eq. 5). The procedure involves the following steps: Step 1: Determine the bending moment distribution (Figure 4Figure 4b), Step 2: Determine the critical moment for each span using the critical moment M_{cr} expressions in Equation 4, where L is the distance between lateral torsional supports (i.e., the left span has $L = 4m$ and the right span has $L = 8m$). Step 3: Determine the critical moments for both spans by applying the quarter-point moment gradient equation (Eq. 5) and conservatively taking the smaller value (i.e., neglecting the interaction between both spans). Table 3 provides a summary of the results. For comparison, FEA predictions are provided for the case where the interaction between both spans is omitted, by modelling each span alone in a separate buckling FEA model while using 8 elements for each span.

Solution (2) - Incorporating interaction effects: The FEA solution provides a natural means of incorporating the interaction between the two spans. This is done by modelling both spans in a single model. For the present problem, this interaction is beneficial for the weaker right span (which governs the design in Solution 1). The stronger left span provides some restraint to left span and delays its buckling. By incorporating interaction effects and using 8 elements for each span, the critical moment of the system is found to increase by 28.6% from the Canadian standards predictions (Table 3). As expected, the artificial isolation of each member leads to overly conservative predictions of the critical moments.

Table 3: Comparison of critical moment predictions for a continuous beam

	Left Span	Right Span	Estimated critical moment for the structure
Bending Moment Diagrams			
Span $L(m)$	4m	8m	
M_u (Eq.4)	386.9 kNm	151.8 kNm	
M_A (kNm)	+5	+5	
M_B (kNm)	+10	+10	
M_C (kNm)	-5	+15	
M_{max} (kNm)	-20	-20	
$C(CAN)$ (Eq.5)	2.219	1.746	
$M_{cr}(CAN) = C(CAN)M_u$ (kNm)	858.5	265.0	265.0
$M_{cr}(FEA)_1$ kNm - neglecting interaction (treating each span in a separate model)	1134	295.1	295.1
$M(FEA)_2$ kNm - accounting for interaction (treating both spans in a single model)		340.7 kNm	340.7

6. CASE STUDY 3: EFFECT OF LATERAL AND TORSIONAL RESTRAINTS AT INTERMEDIATE SUPPORTS

In the previous case study, the middle support was assumed to be laterally and torsionally restrained. In the present example, it is required to investigate the case where intermediate support provides vertical displacement restraint but no lateral nor torsional restraints (Figure 5) as may be the case for a beam supported by a column that is pinned at the base with no lateral members framing into the beam at the beam to column junction. All other loading and end boundary conditions remain unchanged. Since the boundary conditions regarding the transverse displacements are identical to the past case study, the BMD remains identical (Figure 4b). However, in the absence of lateral and torsional restraints at the middle support, the unsupported span of the beam becomes 12m and quarter point moments become $M_A = -5\text{kNm}$, $M_B = +5\text{kNm}$, $M_C = +12.5\text{kNm}$ and $M_{\max} = +20\text{kNm}$. The critical moment calculations based on the Canadian standard equation is found to be 211.2kNm and the steps of the calculation are provided in Table 4. Also, provided for comparison are the critical moments predicted by the FEA which is 191.0 kNm. The Canadian moment gradient equation is found to overestimate the critical moment by 10.5% in this case. A comparison with the previous case study indicates that, although the bending moment distribution remains identical in the two problems, the critical moment is found to drop from $M_{cr} = 340.7\text{kNm}$ for the case where lateral and torsional supports are provided at mid-span to $M_{cr} = 191.0\text{kNm}$ for the case where such restraints are removed.

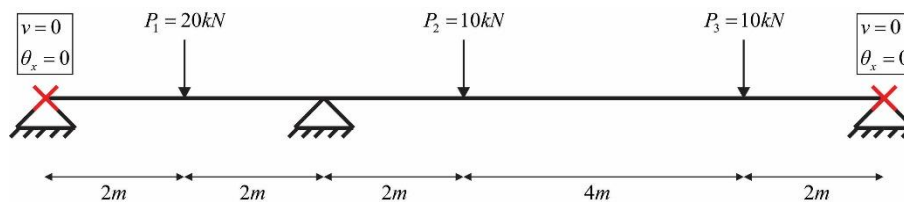


Figure 5: Lateral torsional restraints removed at middle support (Example 3)

Table 4: Critical moment comparisons for Example 3

	Results
Span $L(m)$	12m
$M_u = \frac{\pi}{L} \sqrt{EI_y GJ + \left(\frac{\pi E}{L}\right)^2 C_w J_y}$	95.20
$M_A (kNm)$	-5.0
$M_B (kNm)$	+5.0
$M_C (kNm)$	+12.5
$M_{\max} (kNm)$	-20
$C(CAN)(Eq.5)$	2.219
$M_{cr}(CAN) = C(CAN)M_u (kNm)$	211.2
Finite Element solution $M(FEA)$	191.0

7. CONCLUSIONS

The following conclusions have been drawn from the current study:

1. The present study implemented and established the validity of the beam finite element of Barsoum and Gallagher (1970) as part of a larger project to integrate the element within the commercial S-FRAME analysis software and the S-STEEL steel design software.
2. The formulation was successfully used to derive moment gradient factors in agreement with the Eurocode Guide recommendations and CAN-CSA-S16-14 moment gradient factors. The element was then used to capture interaction effects between adjacent spans when calculating the LTB capacity of continuous beams.
3. Moment gradient factors were proposed for the design of two-span and three-span beams under either mid-span point loads or UDL. The moment gradient factors account for span interaction.
4. The study has quantified the effect of span interaction when determining the elastic LTB resistance. Span interaction was shown to play an important role for three-span beams and two-span beams with unequal spans. In the majority of the cases considered, neglect of interaction effect by adopting the moment gradient factor in the CAN-CSA-S16-14 was shown to lead to conservative predictions of the critical moments.
5. The study quantified the effect of lateral and torsional restraints at intermediate supports. For Case studies 2 and 3, removal of such restraints were shown to result in a significant drop in the critical moments.

8. ACKNOWLEDGEMENTS

The authors wish to express their gratitude to Mr. George Casoli, Dr. Feng Rong, Dr. Siriwut Sasibut, and Dr. Marinos Stylianou, from S-FRAME Software Inc. for their instructive feedback and effort. Financial support from the S-FRAME Software Inc. and matching funds from the Natural Sciences and Engineering Research Council (NSERC) of Canada are also gratefully acknowledged.

9. REFERENCES

- Standards Association of Australia (SAA). 1998, *Steel Structures, AS4100-1998*, SAA, Australian Institute of Steel Construction, Sydney, Australia.
- CSA (2014). "Limit states design of steel structures." *Standard CAN/CSA-S16-14*, Canadian Standards Association, Mississauga, Ontario.
- ANSI/AISC-360-16 (2016). "ANSI/AISC 360-16." *Specification for structural steel buildings*, American Institute of Steel Construction (AISC), Chicago, IL.
- Barsoum, R. S., and Gallagher, R. H. (1970). "Finite element analysis of torsional and torsional-flexural stability problems." *International Journal for Numerical Methods in Engineering*, **2**(3), 335-352.
- Gardner, L., and Nethercot, D. A. (2011). DESIGNERS' GUIDE TO EUROCODE 3: (EN 1993-1-1, -1-3 and -1-8) DESIGN OF STEEL BUILDINGS, Imperial College London, UK.
- Nethercot, D. A., and Trahair, N. S. (1976). "Lateral Buckling Approximations for Elastic Beams." *Structural Engineering*, **54**(6), 197-204.
- Trahair, N. S. (1977). "Lateral Buckling of Beams and Beam-Columns," in *Theory of Beam-Columns*. McGraw-Hill, New York.
- Trahair, N. S., and Bradford, M. A. (1988). *The Behaviour and Design of Steel Structures*, Chapman & Hall, London.
- Vlasov, V. Z. (1961). *Thin-walled elastic beams*, 2nd Edition, Israel Program for Scientific Translation, Jerusalem.
- Ziemian, R. D. (2010). *Guide to stability design criteria for metal structures*, John Wiley & Sons, New York.